IEICE TRANS. ELECTRON., VOL.E87–C, NO.1 JANUARY 2004

PAPER

Improvement in Performance of Power Amplifiers by Defected Ground Structure

Jong-Sik LIM[†a)], ***Member***, **Yong-Chae JEONG**[††], **Dal AHN**[†††], ***and*** **Sangwook NAM**[††††], ***Nonmembers***

SUMMARY This paper describes the performance improvement of power amplifiers by defected ground structure (DGS). Due to the excellent capability of harmonic rejection and tuning, DGS plays a great role in improving the major nonlinear behaviors of power amplifier such as output power, harmonics, power added efficiency (PAE), and the ratio between the carrier and the third order intermodulation distortion (C/IMD3). In order to verify the improvement of performances by DGS, measured data for a power amplifier, which adopts a 30 Watts LDMOS device for the operation at 2.1–2.2 GHz, are illustrated under several operating bias currents for two cases, i.e., with and without DGS attached. The principle of the improvement is described by the simple Volterra nonlinear transfer functions with the consideration of different operating classes. The obtained improvement of the 30 Watts power amplifier, under 400 mA of I_{dsQ} as an example, includes the reduction in the second and third harmonics by 17 dB and 20 dB, and the increase in output power, PAE, and C/IMD3 by 1.3 Watts, 3.4%, and 4.7 dB, respectively.

key words: *defected ground structure, DGS, power amplifiers, harmonic rejection, harmonic tuning*

1. Introduction

The most important design targets of power amplifiers are high output power, efficiency, and excellent linearity. One of the methods to improve the performances is to tune the harmonics at the output [1]–[3]. The second harmonic is especially in want of tuning, because its magnitude is relatively larger than the other harmonics. Previous techniques for tuning harmonics include adding a $\lambda/4$ short-circuited stub [2]–[5] and using a chip capacitor with self-resonance near the second harmonic [6]. Radisic et al. pointed out that the above techniques are narrow band and presented a new method using photonic bandgap (PBG) at the output of the power amplifier [7]. Some improvement was achieved, but drilling for a lot of holes and adding copper tape to the ground plane are required in realizing PBG.

A new technique using defected ground structure (DGS) to improve the performances of power amplifiers was proposed [8]. DGS is another kind of periodic structure, but it is much easier to fabricate because DGS patterns are realized when the amplifier circuit is etched at the same time. Due to the additional, effective L-C components, DGS has a specified passband with low loss and very wide and steep stopband characteristics [9]. To the contrary, in the case of the existing PBGs, the width of stopband is not wide and the slope of the rejection is not steep because the equivalent element is mainly inductive.

If the passband and stopband of DGS are overlapped to the operating frequency band and the harmonic band of power amplifiers, respectively, it is expected that DGS reject not only the second, but also the third and fourth harmonics [8], while the PBG in [7] rejects the second harmonic only. Additionally, if the real part of the input impedance, which are seen to the device, of the output matching network including DGS are zero at harmonic frequencies, it can be said that the harmonics are terminated reactively. This is one of the methods to tune the harmonics for the improved power amplifiers [10].

The previous works showed that the rejection of the harmonic components plays a positive role in improving the output power (P_{out}), power added efficiency (PAE), and harmonic components which appear at output [7], [8], [10]. In this work, the improved linearity of power amplifiers using DGS will be discussed by comparing the measured third order intermodulation distortion products (IMD3) and the ratio between the carrier and IMD3 (C/IMD3) in two-tone test, while the previous works dealt with the results of one-tone test only.

In order to verify the improved performances of power amplifiers by DGS, the power amplifier using a 30 Watts LDMOS device has been fabricated and measured at 2.11–2.17 GHz for two cases, i.e. the power amplifier with DGS at the output section ("WITH DGS") and the power amplifier itself ("WITHOUT DGS"). The test items for comparison are P_{out}, the second and third harmonics at output ($2F_o$, $3F_o$), PAE, IMD3,

Manuscript received August 12, 2002.
Manuscript revised December 10, 2002.

[†]The author is with the Korean Intellectual Property Office, Daejon, Republic of Korea.
[††]The author is with the Division of Electronics and Information Engineering, Chonbuk National University, Chonju, Chonbuk, Republic of Korea.
[†††]The author is with the Division of Information Technology Engineering, SoonChunHyang University, Asan, Chungnam, Republic of Korea.
[††††]The author is with the Applied Electromagnetics Laboratory, Institute of New Media and Communications, School of Electrical Engineering and Computer Science, Seoul National University, Seoul, Republic of Korea.
a) E-mail: jslim@kipo.go.kr

and C/IMD3. Measurements have been performed for several initial bias currents (I_{dsQ}), i.e. several operating conditions, with input power swept. The measured data for two cases will be described and compared with simple Volterra nonlinear transfer functions.

2. The Microstrip Line with DGS on the Ground Plane

Figure 1 shows the general structure of the microstrip line with DGS ("DGS line") proposed in [8] and [9]. The transfer characteristics of the DGS line, depending on the dimensions of the dumb-bell shaped DGS and periodic distance, look like a performance of low pass filters. An important difference in transfer characteristics between PBG in [7] and DGS in [8] is that DGS has a very wide stopband, and no periodic passband exists up to the fourth harmonic, which is considered to be a meaningful harmonic frequency. This means that DGS suppress the higher order harmonics as well as the second harmonic. Theoretically and practically, it is desirable to reject the higher order harmonics, although they are relatively small.

Figure 2 shows the DGS line and the measured properties. DGS line has a compensated width and two DGS patterns on the substrate with 3.48 of dielectric constant and 30 mils of thickness. The dimensions are A=B=5 mm, C=0.5 mm, G=3 mm, W1=1.7 mm, and W2=3.5 mm. W1 is the same as the width of 50-W microstrip line. It is definite that a very wide stopband is observed without any remarkable periodic passband.

The purpose of using DGS is to improve the performance of power amplifiers by suppressing and tuning harmonics. In order to achieve this goal using the minimal number of DGS patterns, two unit DGSs were selected. It is required that the DGS line should have a low loss in the passband and excellent rejection at harmonic bands. If the standard DGS line has some loss at the operating frequency of the power amplifier, it is required to compensate the width of the microstrip line for low loss as in this work, because the large loss at the output of the power amplifier is catastrophic. One additional advantage of the compensated DGS line is that the width of the microstrip line is much wider than that of the conventional microstrip line for the same characteristic impedance due to the increased effective inductive component [11]. This is a great advantage in application where very high power over several tens of Watt-level is handled.

The measured results in Fig. 2 show a typical property of low pass filters (LPF), even though it was not intended to design a LPF at first. The clear differences between the DGS line and the conventional LPF are; 1) much steeper cutoff characteristics, 2) much wider width of microstrip line, i.e. no need for a high impedance line, 3) much smaller size, and so on. The measured small loss at 2.14 GHz means that DGS at

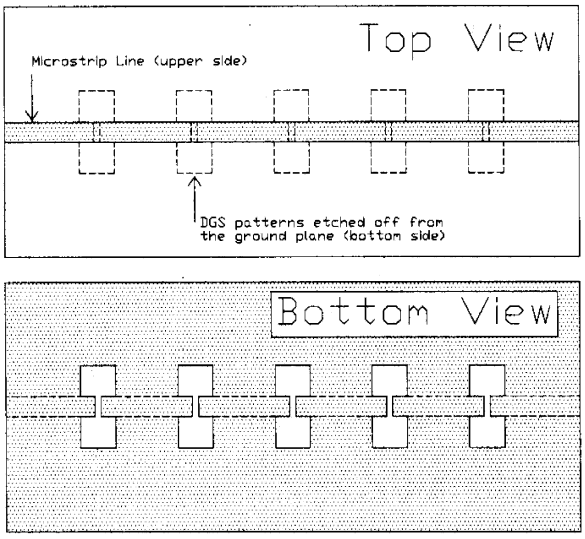

Fig. 1 General structure of a microstrip line with DGS patterns on the ground plane.

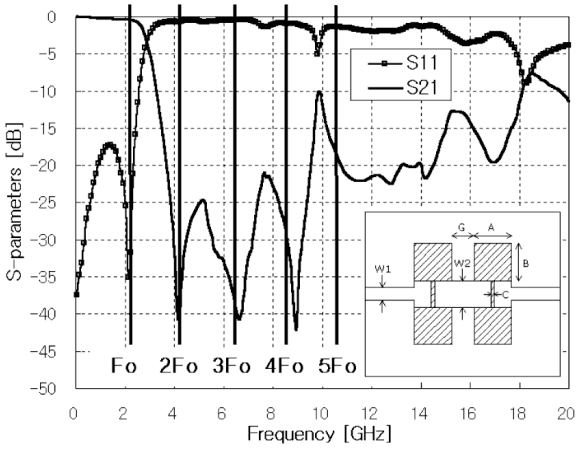

Fig. 2 DGS line used in this work and its measured performance. (F_o=2.14 GHz)

the output of the amplifier rarely reduce linear gain. On the contrary, the slope of the cut-off is very steep and the rejection at harmonic frequencies is excellent. In addition, it should be noted that the ratio between the widths of passband and stopband of Fig. 2 is quite larger than those of other PBG circuits in [7], [12], and [13].

3. Power Amplifier and 1-Tone Measurement

A 30 Watts LDMOS device was adopted to build the power amplifier, which is illustrated in Fig. 3(a). The required drain bias voltage is +28 V. The matching networks are composed of impedance transformer, shunt capacitor, and DC block capacitor. High impedance lines with quarter-wave length are used for bias supply instead of inductor coils. Even though these high impedance lines act like $\lambda/4$ stub for suppressing and

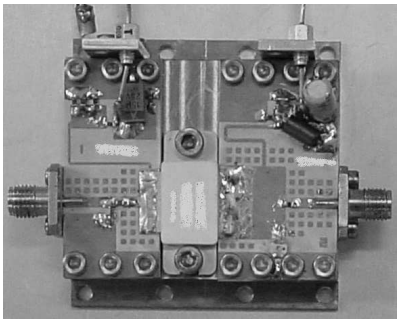

(a)

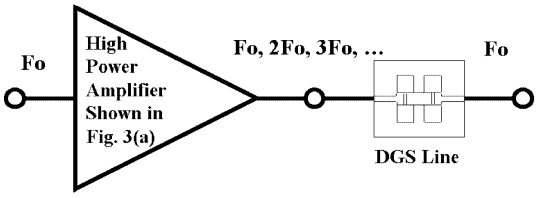

(b)

Fig. 3 (a) The fabricated 30 Watts power amplifier. (b) The power amplifier combined with DGS line.

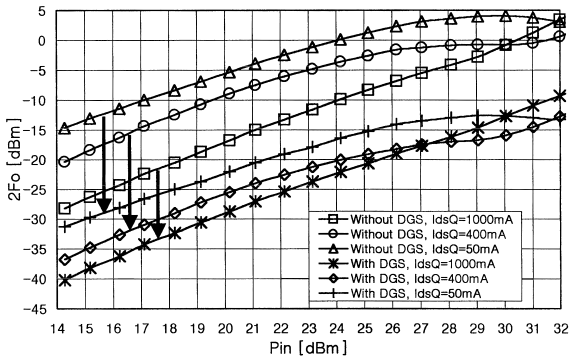

(a)

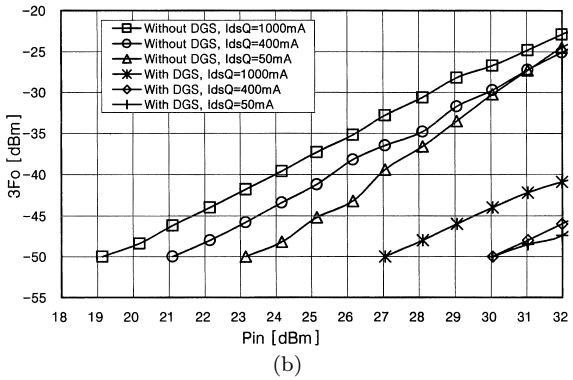

(b)

Fig. 4 Comparison of the measured harmonics under various bias currents. (a) $2F_o$, (b) $3F_o$.

tuning the second harmonic to some degree, it is not sufficient to reject all harmonics perfectly. In practice, the detected levels of the harmonics are never ignorable, despite the $\lambda/4$ high impedance line for bias, in such high power amplifiers over a few decades of Watt, but, in general, considerable second harmonic powers are detected.

The key concept of this work is shown briefly in Fig. 3(b). The fundamental (F_o) and nth harmonic components (nF_o, $n = 2, 3, ...$) at the output are faced with DGS line. Only the fundamental component passes it, the other harmonics are reflected back into the device and cause the fundamental power to increase [4].

In order to investigate the performance improvement by DGS, the power amplifier was measured under several operating classes by adjusting I_{dsQ}. The firstly applied bias current for the device is 400 mA, which has been estimated as the I_{dsQ} for the operating class between AB and A by the measured nonlinear behaviors of the power amplifier. The 1000 mA of I_{dsQ} is far beyond the current for the normal class A operation. The operating class is defined as a class B in this work when I_{dsQ} is 50 mA, although it is slightly higher than the current for the ideal class B operation.

The performance improvement under three I_{dsQ}s has been verified through the measurement with input power swept. Figures 4(a) and (b) show the measured second and third harmonic powers under three bias currents. The reduction of the second and third harmonics amounts to 17 dB and 20 dB, respectively. The reduction of harmonics is observed definitely under all operating classes. It is seen clearly that a $\lambda/4$ stub is not sufficient for suppression all harmonics.

The reduction of the second harmonic depends on the operating class. It is observed that the higher I_{dsQ}, the relatively smaller improvement in Fig. 4(a). This can be explained by considering the general properties of power amplifiers. In general, the second harmonic increases as the I_{dsQ} decreases because the distortion of the signal is getting severe. Therefore the improvement of the second harmonic by DGS is the best in the case of the smallest I_{dsQ}.

It is expected that the suppression of harmonics will lead the improvement in other performances such as Pout and PAE. Figures 5(a) and (b) show the measured Pout and PAE. To make the figures brief and readable, the measured results are illustrated here only for three inputs, 20, 27, and 30 dBm. From Fig. 5(a), it is evident that the output power of "WITH DGS" is greater than that of "WITHOUT DGS" for all operating classes. The resultant improved PAE is illustrated in Fig. 5(b).

Figures 6(a) and (b) show the comparison of the measured data in order to quantify the improvement. The output power has been improved by 0.16–0.65 dBm, 0.37–0.75 dBm, and 0.14–0.68 dBm for 50 mA, 400 mA, and 1000 mA of I_{dsQ}, respectively. These improvements correspond to the higher output powers by 0.2–1.3 Watts. The resultant PAEs of "WITH DGS" are greater than that of "WITHOUT DGS" by 0.4–1.92%, 0.56–3.39%, and 0.41–2.65%, re-

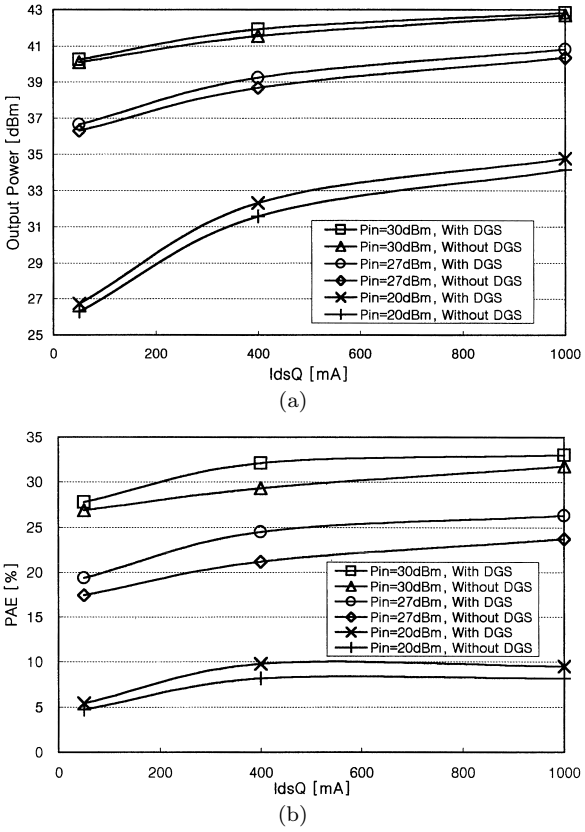

Fig. 5 Comparison of the performances for two cases. (a) Output power, (b) power added efficiency.

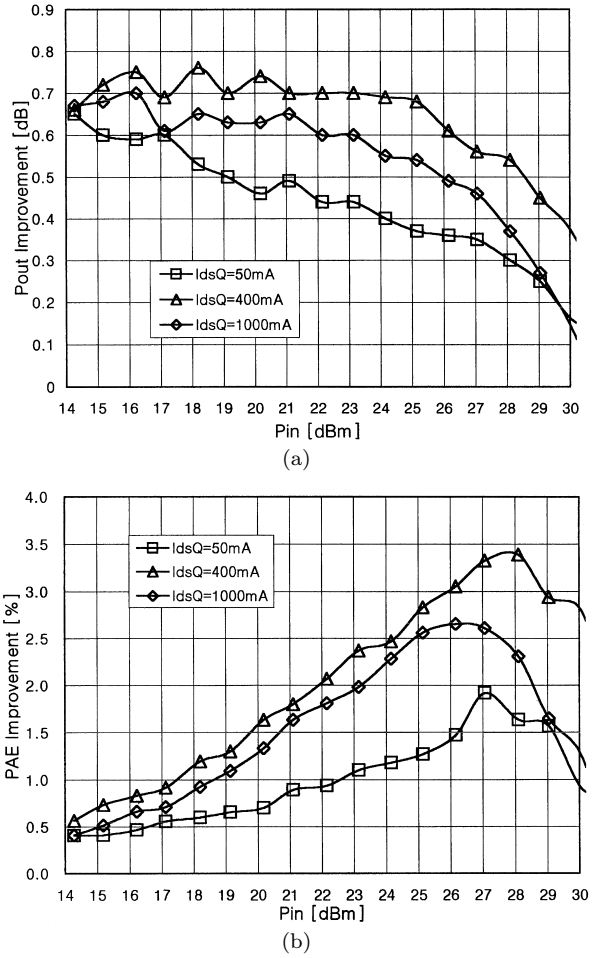

Fig. 6 The quantities of improvement by DGS under various operating classes by adjusting I_{dsQ}. (a) Output power, (b) power added efficiency.

spectively.

It is noted that the PAE improvement under 50 mA of I_{dsQ} is smaller than those of other bias currents, while the relative improvement of rejecting the second harmonic is the best one. Although the generated second harmonic under 50 mA of I_{dsQ} is the largest one as shown in Fig. 4(a), it should be noted that the absolute magnitude of the output power is the smallest as shown in Fig. 5(a), and the relative improvement of output power by DGS is the smallest one as shown in Fig. 6(a). Generally, the dominant factor(s) for high PAE is the high output power or small DC current (under a fixed DC voltage) or both of them. In this case, it is believed that the improvement of output power under high I_{dsQ} operations is lager than that of 50 mA of I_{dsQ}. For such very high power amplifiers with a few decades of Watt or more, the increase of only a few tens of dB, for example, 0.3–0.7 dB in Pout in this work, produce the increase of a few Watts in the output power and a few % in the PAE. So, it is thought that the rejected second harmonic under 50 mA of I_{dsQ} leads to the relatively smaller increase of Pout than other bias currents.

It has been reported that the efficiency of power amplifiers depends on the harmonic termination directly [5], [10], [14]. Figures 7 (a) and (b) show the impedances, which are seen to the device, of output matching network itself and output matching network combined by the DGS line. It is observed that the termination impedance at $2F_o$ frequency moves to near the ideal short point by attaching DGS line, even though $4F_o$ is still located at a point far away from ideal short. It can be argued that the second, third, and fourth harmonics are terminated reactively, because the real parts are zero, although the effect of the termination impedance at $4F_o$ is expected to be not sensitive to efficiency. In summary, the second and third harmonics are not only rejected, but also reactively terminated by DGS.

4. Two-Tone Measurement and IMD3 Improvement by DGS

In the above section, it has been described that the improvement in output power, harmonics, and power added efficiency have been obtained under all bias currents by combining DGS to output matching network. Based on the improvements, we are going to show the

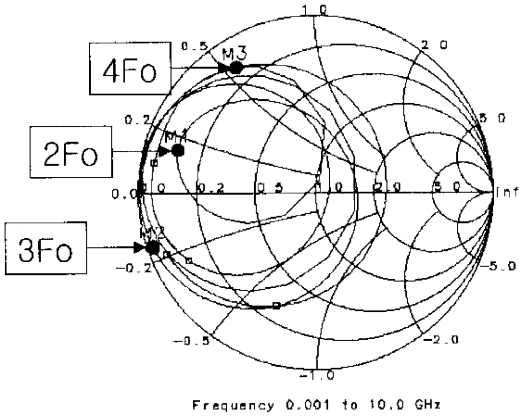

(a)

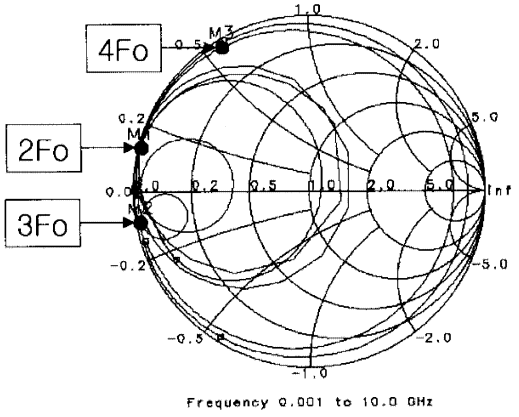

(b)

Fig. 7 Termination impedances seen to the device at harmonic frequencies. M1, M2, and M3 indicate the 2nd, 3rd, and 4th harmonic frequencies, respectively. (a) Output matching only, (b) output matching combined DGS line.

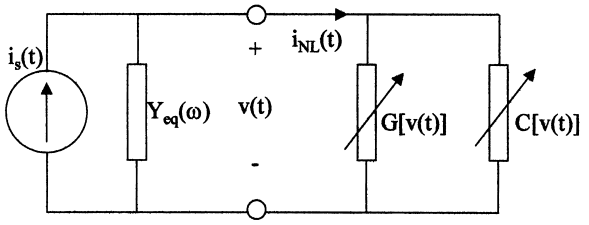

Fig. 8 Simplified nonlinear circuit for IMD analysis. DGS is incorporated into $Y_{eq}(\omega)$.

reduction of IMD3 in two-tone test. Figure 8 represents the generally used, simplified nonlinear circuits for IMD3 analysis. Using the basic circuit concepts, it is possible to define the current source, internal equivalent impedance, and nonlinear resistive and reactive loads [15], [16].

In a strict premise in the analysis using nonlinear transfer function, DGS is just a passive element, and $G[v(t)]$ and $C[v(t)]$ are strongly dependent on bias only. However in a real situation, $G[v(t)]$ and $C[v(t)]$ are also functions of $v(t)$, and $v(t)$ is influenced by the termination impedance, $Z_{eq}(\omega)$. Again, $Z_{eq}(\omega)$ is determined by the passive part including the equivalent passive elements in device, the output matching network, and DGS line. Once the design is finished and the output matching network is fabricated, $Z_{eq}(\omega)$ of the passive part, except DGS line, is fixed. In other word, DGS line changes $Z_{eq}(\omega)$ to a new value. Therefore $G[v(t)]$ and $C[v(t)]$ are affected if the DGS line is attached to the output matching network.

One more important fact is that the harmonic power reflected back into the device depends on the existence of DGS line, because $Z_{eq}(n\omega)$, where $n = 2, 3, 4, \cdots$, changes if DGS line is combined to the output matching network. Because the nonlinear transfer functions are also dependent upon the $Z_{eq}(n\omega)$, attaching DGS line is one of the causes which change the nonlinear behavior of power amplifiers, even though the precise analysis has not been developed quantitatively yet.

The components of the nonlinear current can be expressed like Eq. (1). In a linear or weakly nonlinear region, G_2 and C_2 are dominant over G_3 and C_3. When the input and output are $i_s(t)$ and $v(t)$ respectively, the Volterra nonlinear transfer functions up to the third order can be expressed as Eqs. (2)–(4) for one-tone input signal [16].

$$i_{NL}(t) = \left[G_2 + \frac{\partial}{\partial t}C_2\right] v^2(t) + \left[G_2 + \frac{\partial}{\partial t}G_3\right] v^3(t) \tag{1}$$

$$H_1(\omega) = \frac{1}{Y_{eq}(\omega)} = Z_{eq}(\omega) \tag{2}$$

$$H_2(\omega, \omega) = -Z_{eq}(2\omega)[G_2 + j2\omega C_2][{H_1}^2(\omega)] \tag{3}$$

$$\begin{aligned} H_3(\omega, \omega, \omega) = {} & \frac{-Z_{eq}(3\omega)}{6}\{2[G_2 + j3\omega C_2] \\ & \cdot [3H_1(\omega)H_2(\omega, \omega)] + 6[G_3 + j3\omega C_3][{H_1}^3(\omega)]\} \end{aligned} \tag{4}$$

Provided that 2-tone input signals, ω_1 and ω_2, are injected into the power amplifier with the same magnitude, it is possible to express the input signal as $i_s(t) = e^{j\omega_1 t} + e^{j\omega_2 t}$. At frequencies $(2\omega_2 - \omega_1)$ and $(2\omega_1 - \omega_2)$, the IMD3 components can be described as follows.

For $(2\omega_1 - \omega_2)$,

$$\begin{aligned} H_3(\omega_1, \omega_1, -\omega_2) = {} & \frac{-Z_{eq}(2\omega_1 - \omega_2)}{6} \\ & \cdot \Big\{2[G_2 + j(2\omega_1 - \omega_2)C_2][H_1(-\omega_2)H_2(\omega_1, \omega_1) \\ & + 2H_1(\omega_1)H_2(-\omega_2, \omega_1)] \\ & + 6[G_3 + j(2\omega_1 - \omega_2)C_3][{H_1}^2(\omega_1)H_1(-\omega_2)]\Big\} \end{aligned} \tag{5}$$

and for $(2\omega_2 - \omega_1)$,

$$H_3(\omega_2, \omega_2, -\omega_1) = \frac{-Z_{eq}(2\omega_2 - \omega_1)}{6}$$

$$\cdot \Big\{ 2[G_2 + j(2\omega_2 - \omega_1)C_2][H_1(-\omega_1)H_2(\omega_2, \omega_2) + 2H_1(\omega_2)H_2(-\omega_1, \omega_2)] + 6[G_3 + j(2\omega_2 - \omega_1)C_3][{H_1}^2(\omega_2)H_1(-\omega_1)] \Big\} \quad (6)$$

It can be said that the magnitudes of $H_2(\omega, \omega)$ and $H_3(\omega, \omega, \omega)$ have been reduced by DGS because of the decreased second and third harmonics. Considering Eqs. (3) and (4), the reduction is directly related to the reduction of G_2, C_2, G_3, and C_3, even though it can be said that $H_1(\omega)$ has increased because of the improved fundamental output power. However, it is concluded that the relative reduction of G_2, C_2, G_3, and C_3 is dominant over the relative increase of $H_1(\omega)$, because $H_2(\omega, \omega)$ and $H_3(\omega, \omega, \omega)$ have been substantially reduced.

It is possible to explain the reduced magnitudes of $H_2(\omega, \omega)$ and $H_3(\omega, \omega, \omega)$ from another point of view. $H_2(\omega, \omega)$ and $H_3(\omega, \omega, \omega)$ also have dependency on $Z_{eq}(2\omega)$ and $Z_{eq}(3\omega)$ as shown in Eqs. (3) and (4). So it can be said that the relative reduction of $Z_{eq}(2\omega)$ and $Z_{eq}(3\omega)$ is dominant over the relative increase of $H_1(\omega)$, because of the quite reduced $H_2(\omega, \omega)$ and $H_3(\omega, \omega, \omega)$.

Now, the improvement, i.e. reduction of IMD3 by DGS can be explained. The third order nonlinear transfer functions are dependent on G_2, C_2, G_3, C_3, $H_1(.)$, and $H_2(.,.)$. The rejection of harmonics decreases not only G_2 and C_2, but G_3 and C_3. In addition, $H_2(.,.)$ has been reduced. Therefore, in (5) and (6), the reduction of G_2, C_2, G_3, C_3, and $H_2(.,.)$ is relatively dominant over the slight increase of $H_1(.)$. However, in this case, the role of $Z_{eq}(2\omega_1 - \omega_2)$ and $Z_{eq}(2\omega_2 - \omega_1)$ is weak, because they are expected to be similar to $Z_{eq}(\omega)$ if the tone space is very narrow. So any change of them by DGS, if there is, will not be critical in determining $H_3(.,.,.)$.

Figure 9 and Fig. 10 show the measured C/IMD3 and the reduced quantities of IMD3 for three I_{dsQ}s. The C/IMD3 improvement is observed for all operating classes as has been expected through the nonlinear transfer functions and the related description above. The IMD3 sweet spot, which is a typical phenomenon of class B operation [17], is observed.

It is interesting to compare the reduction of IMD3 versus bias. Before discussing it, some considerations should be noted first. 1) The fundamental output power under 50 mA of I_{dsQ} is the smallest, while the distortion is the most severe. 2) In general, the normal class A operation produces the highest output power with the smallest distortion. 3) In this work, the 1000 mA of I_{dsQ} is a much higher operating point than normal class A. The swing of the signal will stay in linear region first, and goes into distortion as the input power increases and gets closer to the saturation when the I_{dsQ} is 1000 mA. 4) Because G_2, C_2, G_3, and C_3 are strongly bias dependent, they are smaller in normal class A or AB than class B and beyond class A.

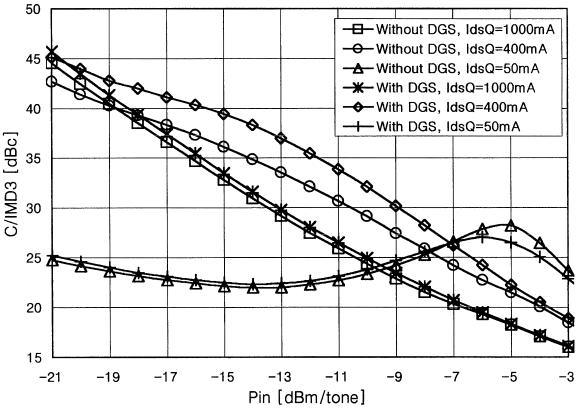

Fig. 9 The improved C/IMD3 by DGS. (Two identical, class A amplifiers with 32dB of gain and 3 Watts of output power were used as driver amplifiers.)

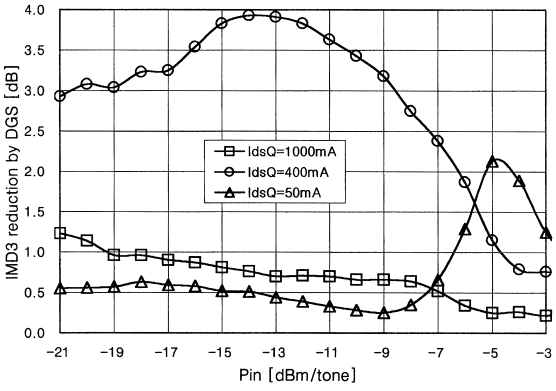

Fig. 10 The reduction of IMD3 by DGS. The maximum reduction of 4 dB corresponds to the improvement of 4.7 dB in C/IMD3 because the fundamental has improved by 0.7 dB in Fig. 6(a).

Even though G_2, C_2, G_3, and C_3 have been reduced by DGS, the relative magnitudes of G_2, C_2, and $H_2(.,.)$ at 50 mA of I_{dsQ} are still higher than the other classes, because the measured second harmonic power is still the largest as shown in Fig. 4(a). So the first terms in the braces of Eqs. (5) and (6) are still dominant in determining IMD3. Hence, it is understood that the relative improvement of IMD3 at 50 mA of I_{dsQ} is the smallest in Fig. 10.

It may be expected that the IMD3 improvement under 1000 mA of I_{dsQ} should be better than or at least equal to that at 400 mA. However, contrary to this expectation, the IMD3 improvement at 1000 mA shown in Fig. 10 is poorer than 400 mA. The reason is that 1000 mA is not the quiescent condition of normal class A, but is beyond class A. This non-optimum biasing point causes early voltage clipping of waveform by knee voltage of the device, and leads to a severely distorted operation as opposed to normal class A operation. The improvement of IMD3 at 1000 mA gives

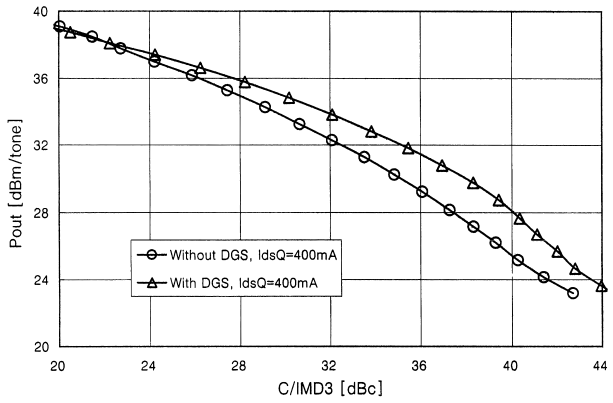

Fig. 11 Comparison of output powers of the 30 Watts power amplifier for the fixed C/IMD3.

us one clue related to the estimation of the operating class of this device. The improvement degrades slightly as the input goes up, because intermodulation distortion products increase rapidly while the fundamental output power saturates. This verifies that 1000 mA is beyond the quiescent current of normal class A.

It is significant to compare the output power for the same level of C/IMD3, because this is one of the barometers for the linearity of power amplifiers, especially in a base station of digital communication systems. It is desirable that the output power be as high as possible for a fixed level of C/IMD3 for better linearity in power amplifier itself so that the burden of linearization can be mitigated. Figure 11 shows that the power amplifier with DGS operates more linearly than the case of "WITHOUT DGS."

5. Conclusion

A new method for improving the performance of power amplifiers by suppressing and tuning the harmonics using DGS has been proposed. It was shown by measurement that the DGS line has a very broad stopband, which includes several harmonic frequencies. The measured performances such as harmonic suppression, output power, power added efficiency, harmonic rejection, and IMD3 were discussed under various biases for two cases; the power amplifier with and without DGS combined to the output section.

The obtained improvement by DGS from the power amplifier using a 30 Watts LDMOS, under 400 mA of I_{dsQ} as an example, includes the reduction in the second and third harmonics by 17 dB and 20 dB, and the increase in output power and PAE by 1.3 Watts and 3.4%, respectively.

The IMD3 improvement in two-tone test has been described using a simplified equivalent nonlinear circuit and related nonlinear transfer functions. In order to show that the improvement of IMD3 depends on the operating classes, the power amplifier has been measured under three bias currents for two cases. The improvement of IMD3 under 400 mA of I_{dsQ} was measured by 4 dB.

The DGS line is separated from the power amplifier intentionally in this work to compare the performance for two cases, "WITH DGS" and "WITHOUT DGS," because, to our knowledge, this is the first attempt to improve the performances of the power amplifier with a few tens Watt-level using DGS under various operating classes. However, it is easy to incorporate DGS to the 50-Ω line at output matching network. It is expected that the proposed technique is well applicable to other kinds of power amplifiers using MIC, in MMIC and RFIC technologies.

Acknowledgements

This work was supported by the Brain Korea 21 Project.

References

[1] J.L.B. Walker, High-Power GaAs FET Amplifiers, pp.210–212, Artech House, Norwood, MA, 1993.
[2] S.C. Cripps, RF Power Amplifiers for Wireless Communications, pp.88–90, Artech House, MA, 1999.
[3] S. Mazumder, A. Azizi, and F. Gardiol, "Improvement of a class-C transistor power by the second-harmonic tuning," IEEE Trans. Microw. Theory Tech., vol.MTT-27, no.5, pp.430–433, May 1979.
[4] J. Lane, R. Freitag, H.-K. Hahn, J. Degenford, and M. Cohn, "High-efficiency 1-, 2-, and 4-W class-B FET power amplifiers," IEEE Trans. Microw. Theory Tech., vol.MTT-34, no.12, pp.1318–1326, Dec. 1986.
[5] C. Duvanaud, S. Dietsche, G. Pataut, and J. Obregon, "High-efficiency class F GaAs FET amplifier operating with very low bias voltage for use in mobile telephones at 1.75 GHz," IEEE Microw. Guid. Wave Lett., vol.3, no.8, pp.268–270, Aug. 1993.
[6] E. Camargo and R.M. Steinberg, "A compact high power amplifier for handy phones," IEEE MTT-S Int. Microwave Symposium Digest, pp.565–568, 1994.
[7] V. Radisic, Y. Qian, and T. Itoh, "Broad power amplifier using dielectric photonic bandgap structure," IEEE Microw. Guid. Wave Lett., vol.8, no.1, pp.13–14, Jan. 1998.
[8] J.S. Lim, H.S. Kim, J.S. Park, D. Ahn, and S. Nam, "A power amplifier with efficiency improved using defected ground structure," IEEE Microw. Wireless Component Lett., vol.11, no.4, pp.170–172, April 2001.
[9] C.S. Kim, J.S. Park, D. Ahn, and J.B. Lim, "A novel 1-D periodic defected ground structure for planar circuits," IEEE Microw. Guid. Wave Lett., vol.10, no.4, pp.131–133, April 2000.
[10] C.Y. Hang, Y. Qian, and T. Itoh, "High efficiency S-band class AB push-pull power amplifier with wide band harmonic suppression," IEEE MTT-S Int. Microwave Symposium Digest, pp.1079–1082, 2001.
[11] D. Ahn, J.-S. Park, C.-S. Kim, J. Kim, Y. Qian, and T. Itoh, "A design of the low-pass filter using the novel microstrip defected ground structure," IEEE Trans. Microw. Theory Tech., vol.49, no.1, pp.86–93, Jan. 2001.
[12] F.-R. Yang, K.-P. Ma, Y. Qian, and T. Itoh, "A uniplanar compact photonic-bandgap (UC-PBG) structure and

its applications for microwave circuits," IEEE Trans. Microw. Theory Tech., vol.47, no.8, pp.1509–1514, Aug. 1999.
[13] A.S. Andrenko, Y. Ikeda, and O. Ishida, "Application of PBG microstrip circuits for enhancing the performance of high-density substrate patch antennas," Microw. Opt. Tech. Lett., vol.32, no.5, pp.340–344, March 2002.
[14] J.E. Mueller, U. Gerlach, G.L. Madonna, M. Pfost, R. Schultheis, and P. Zwicknagl, "A 3 V small chip size GSM HBT power MMIC with 56 percent PAE," Microwave Journal, April 2001.
[15] S.A. Maas, Nonlinear Microwave Circuits, pp.172–199, Artech House, Norwood, MA, 1988.
[16] N.B. Carvalho and J.C. Pedro, "Two-tone IMD asymmetry in microwave power amplifiers," IEEE MTT-S Int. Microwave Symposium Digest, pp.445–448, 2000.
[17] N.B. Carvalho and J.C. Pedro, "Large signal IMD sweet spots in microwave power amplifiers," IEEE MTT-S Int. Microwave Symposium Digest, pp.517–520, 1999.

Jong-Sik Lim received the B.S. and M.S. degrees in electronic engineering from Sogang University, Seoul, Republic of Korea, in 1991 and 1993, and Ph.D. degree from the school of electrical engineering and computer science, Seoul National University in 2003. He joined Electronics and Telecommunications Research Institute (ETRI), Daejeon, Republic of Korea, in 1993 and was with them for 6 years in Satellite Communications Division as a senior member of research staff. He was a key member in developing MMIC LNA and SSPA for the 20/30 GHz satellite transponder in ETRI. From March to July 2003, he was with the Division of Information Technology, Brain Korea 21 Project in Seoul National University, as a member of post doctoral fellow. He gave lectures in the graduate schools of Soonchunhyang University and Soongsil University during the first semester, 2003. Since July 2003, he has been with the Korean Intellectual Property Office. His current research interests include design of the passive and active circuits for RF/microwave and millimeter-wave with MIC/MMIC technology, modeling of active device, design of high power amplifiers, applications of periodic structure to the RF/microwave circuits and modeling of passive structure having periodic structures.

Yong-Chae Jeong received the BSEE and MSEE degrees in electronic engineering from Sogang University, Seoul, Republic of Korea, in 1989 and 1991, respectively. From 1991 to 1998, he worked as a senior engineer with Samsung Electronics. In 1996, he received the Ph.D. in electronic engineering from Sogang University. In 1998, he joined division of electronics and information engineering, and institute of information and communication in Chonbuk National University, in Chonju, Republic of Korea. Now he is an associate professor and currently teaching and conducting research in the area of microwave devices, base-station amplifiers, and linearizing technology.

Dal Ahn received the B.S., M.S., and Ph.D. degrees in electronic engineering from Sogang University, Seoul, Republic of Korea, in 1984, 1986, and 1990, respectively. From 1990 to 1992, he was with the Mobile Communications Division, Electronics and Telecommunications Research Institute (ETRI), Daejeon, Republic of Korea. Since 1992, he has been with the School of electrical and electronic engineering, Soonchunhyang University, Asan, Chungnam, Republic of Korea, where he is currently a associate professor. He is currently Chief of RF and microwave component research center (RAMREC), Soonchunhyang University. His current research interests include the design and application of passive and active components at radio and microwave frequencies, and circuit modeling. He is technical consultant of TelWave Inc. and MRW Technologies, Republic of Korea.

Sangwook Nam received the B.S. degree from the Seoul National University, Seoul, Republic of Korea, in 1981, the M.S. degree from the Korea Advanced Institute of Science and Technology, Republic of Korea, in 1983, and the Ph.D. from the University of Texas at Austin, in 1989, all in electrical engineering. From 1983 to 1986, he was a researcher at Gold Star Central Research Laboratory, Seoul, Korea. Since 1990, he has been with Seoul National University, where he is currently a Professor in the School of Electrical Engineering and Computer Science. His research interests include analysis/design of electromagnetic (EM) structures, antennas and microwave active/passive circuits.